Nanometric optical tweezers based on nanostructured substrates

A. N. GRIGORENKO*, N. W. ROBERTS, M. R. DICKINSON AND Y. ZHANG

School of Physics and Astronomy, University of Manchester, Manchester M13 9PL, UK
*e-mail: sasha@manchester.ac.uk

Published online: 11 May 2008; doi:10.1038/nphoton.2008.78

The ability to control the position of a mesoscopic object with nanometric precision is important for the rapid progress of nanoscience. One of the most promising tools to achieve such control is optical tweezers, which trap objects near the focus of a laser beam. However, the drawbacks of conventional tweezers include a trapping volume that is diffraction-limited and significant brownian motion of trapped nanoobjects. Here, we report the first experimental realization of three-dimensional nanometric optical tweezers that are based on nanostructured substrates. Using electromagnetically coupled pairs of gold nanodots in a standard optical tweezers set-up, we create an array of subwavelength plasmonic optical traps that offer a significant increase in trapping efficiency. The nanodot optical near-fields reduce the trapping volume beyond the diffraction limit and quench brownian motion of the trapped nanoparticles by almost an order of magnitude as compared to conventional tweezers operating under the same trapping conditions. Our tweezers achieve nanoscale control of entities at significantly smaller laser powers and open new avenues for nanomanipulation of fragile biological objects.

Different branches of nanoscience have benefited strongly from robust methods of object manipulations[1–4]. For example, the continued development of optical trapping[4] has seen this technique become one of the most important modern-day tools for research in the fields of biology, physical chemistry and soft condensed matter physics[5], regularly delivering new insights and discoveries[6,7]. The technique's broad appeal has come about because of its non-contact nature—a nano- or microscopic object can be picked up, delivered to a desired place in order to facilitate the act of a measurement or reaction, and then brought back to an initial pool. Recently, the possibilities of such integrated particle manipulation and measurement have been expanded upon with the use of automated systems[8].

Conventional optical tweezers trap objects near the focus of a laser beam. As a result, the trapping volume of conventional tweezers is diffraction-limited, and trapped nanoobjects are often exposed to prominent brownian motion. Several works have shown that conventional optical tweezers still allow one to suppress this brownian motion and to achieve nanometric accuracy of optical trapping (in relatively low bandwidth) by increasing the power of the laser beam, optimizing the sample properties or by using particles with a high polarizability[9–11]. However, these refinements are not appropriate for many systems, particularly for interesting biological samples where the object's polarizability is low and strong laser radiation could cause damage. For these reasons, nanometric trapping of bio-objects requires a rather complicated optical set-up[12].

The diffraction limit is not a fundamental restriction[13], but rather is heuristic, which has been surpassed in several areas of optics with the help of light wavefronts carefully sculptured by artificial nanostructures[14–17]. For example, the trapping volume could be reduced beyond the diffraction limit using optical near-fields[18–20]. Theoretical nanometric optical tweezers[19] rely on strongly enhanced electromagnetic fields near metallic nanoparticles and offer a subwavelength trapping volume. So far, the subwavelength size of an optical trap has been experimentally realized only in one dimension using surface plasmon resonance on a flat gold film[21–23] or focused evanescent wave illumination[24].

In this work, we describe the first experimental realization of using strongly enhanced and localized near-fields of metallic nanostructures of a specially chosen design to produce three-dimensional nanometric optical tweezers with a subwavelength size for the optical trap and strongly enhanced trapping efficiency.

RESULTS

PROPOSED APPROACH

The subwavelength optical traps were produced near the surface of arrays of gold nanoparticles fabricated by high-resolution electron beam lithography on a glass substrate. Instead of a single sharply pointed pin[19], we made use of nanomolecules formed by gold nanodots arranged in tightly spaced pairs. Such a geometry provides excellent control over the critical feature (the gap in the pair) and the frequencies of the localized plasmon resonances[14,25–28], which can be excited by light of normal incidence. It also yields a subwavelength three-dimensional-trap, which is a step forward from previous experiments[21–24].

To demonstrate the action of nanometric optical tweezers, solid polystyrene beads (6 μm, 1 μm and 200 nm in diameter, refractive index of 1.6) were trapped and nanomanipulated by a focused laser beam at controlled focal distances from the surface of the nanostructured substrate, submerged into an immersion oil of refractive index $n = 1.5$. We chose oil in place of water in order to simplify the set-up to the greatest extent possible. Also, the strong dependence of oil viscosity on temperature allowed us to

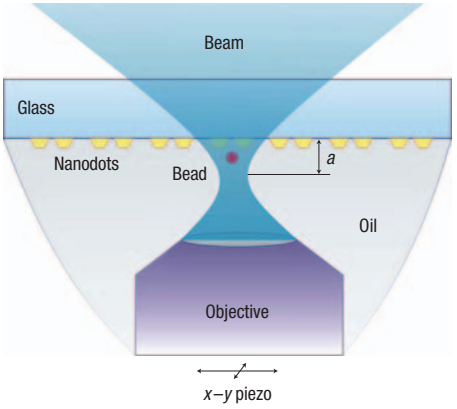

Figure 1 Nanotweezers set-up. Schematics of the laser tweezer installation based on a nanostructured substrate.

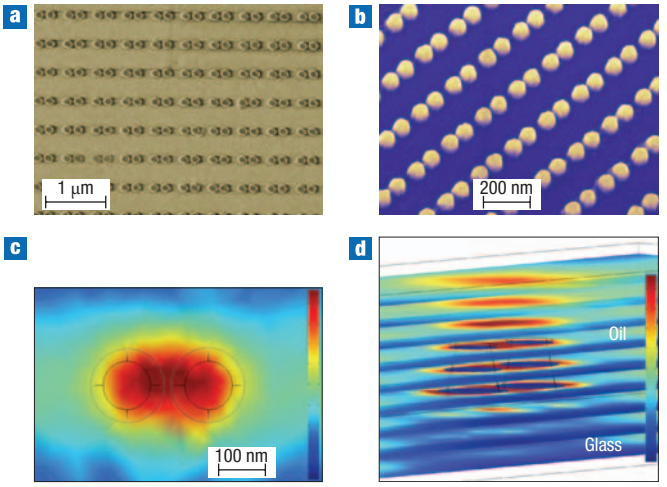

Figure 2 Nanostructured substrates. a, Micrograph of a sample with dot average diameters $D = 134$ nm (pair separation $s = 200$ nm, lattice constant $c = 500$ nm and height $h = 90$ nm). **b**, Micrograph of the sample with a smaller lattice constant obtained under a tilted angle in false colour. **c**,**d**, Light power excited by transverse-magnetic laser light (1,064 nm) of power P_0 is shown as a colour map and calculated for a plane at a height 200 nm above the nanostructured substrate (the plane is parallel to the glass substrate) (**c**), plane slices parallel to the glass substrate and separated by an interval of 50 nm (**d**). The colour map ranges from P_0 to 30 P_0.

check if heating affected our results (see below). The experimental set-up has been described previously[29] and is outlined briefly in the Methods. Figure 1 shows a schematic diagram of the nanotweezers set-up. The trap was created using a continuous-wave 1 W, 1,064 nm neodymium-doped YVO_4 diode pumped solid-state laser, collimated to a beam diameter of 5 mm and focused through an oil-immersion objective of numerical aperture NA = 1.3 onto the sample[29]. The studied structures were placed on a motorized x–y translation stage with a position resolution of 20 nm. The trapping was simultaneously studied with both a charge-coupled device (CCD) camera to visually monitor the trapped particle and a quadrant photodiode (here an additional He–Ne 632.8 nm laser was used to track the particle) to measure its x–y position with a resolution of 0.5 nm $Hz^{-0.5}$.

Figure 2a,b show electron micrographs of the nanostructured samples. The samples were regular square two-dimensional arrays of nanodots grouped in tightly spaced pairs, which covered an area of 0.4 mm × 0.4 mm. Heights h of the gold dots (nanopillars) and their diameters D were chosen through numerical simulations so that the localized plasmon resonance of an individual pillar appeared at deep red and near infrared light frequencies[14]. The data described here were obtained on six samples with the same pair separation $s = 200$ nm, a lattice constant of $c = 500$ nm and height $h = 90$ nm, but different diameters of the nanodots. At such small dot separations, the electromagnetic interaction between nanodots[14,25–28] splits the localized plasmon resonance of an individual nanopillar into two resonances for the pillar pair, and localized plasmon modes of the double pillar nanomolecule can be characterized by their parity[14,26]. In our experiments, the symmetric plasmon resonance of the double-pillar nanomolecule was excited by the infrared laser light ($\lambda = 1{,}064$ nm) and generated the strong electromagnetic fields required for operation of the nanometric tweezers. It has to be noted that the localized plasmonic resonances for nanopillars covered in immersion oil are broad (with half-width >200 nm), and the nanodot near-fields are amplified and generate a strong optical trap even well outside the resonance position[30]. The gaussian laser beam coming from the objective had a diameter of $2\lambda/(\pi \cdot \mathrm{NA}) \approx 500$ nm and on average illuminated just one pillar pair. The trapping position of the beam was produced by a superposition of the gaussian beam profile with strongly localized near-fields generated by the nanodots. When the beam was moved along the nanodot lattice, the trap position varied in space periodically. Figure 2c,d shows cross-sections of the electromagnetic field intensity of near-fields excited by the 1,064 nm light wavefront and calculated for the actual experimental geometry using Femlab software. The electromagnetic field intensity provides a rough guide for the trapping force due to the near-fields. The actual force can be found by integrating the Maxwell stress tensor for the electromagnetic field distribution (calculated in the presence of the bead) over the area surrounding the bead. These calculations suggest that the double-pillar nanomolecules could yield a near-field trap with a typical size of ~100 nm and offer an amplification of the trapping force by almost two orders of magnitude near the nanostructured surface. In comparison with a single dot[19], the double-pillars geometry provides a better control of the nanocavity 'volume' of fabricated nanomolecules and the bigger field enhancements.

OPTICAL TRAPPING AND MANIPULATION OF NANO-SIZED OBJECTS

Figure 3 shows the main experimental result of the paper—optical trapping of 200 nm beads near the nanostructured substrates. In these experiments the focal point of the laser beam was moved parallel to the surface in the symmetry plane of the nanopillar pair at a distance a from the surface. At $a = 14$ μm a 200 nm bead follows the focal point of the beam as shown in Fig. 3a, which plots an average position of the bead (bandwidth of 100 Hz). The situation changes radically when the light is focused closer to the substrate and the distance a is decreased to $a = 0.7$ μm (Fig. 3b). In this case, the motion of a trapped 200 nm bead is dominated by near-fields of nanodots and a bead moves in a step-like manner from one stable trapping point generated by near-fields of an illuminated nanodot pair to the next illuminated pair as the laser beam is moved along the nanodot array. Remarkably, the trapping length scale (evaluated from the change of particle position between the plateaus of Fig. 3b) was well below 100 nm for the stable points, which

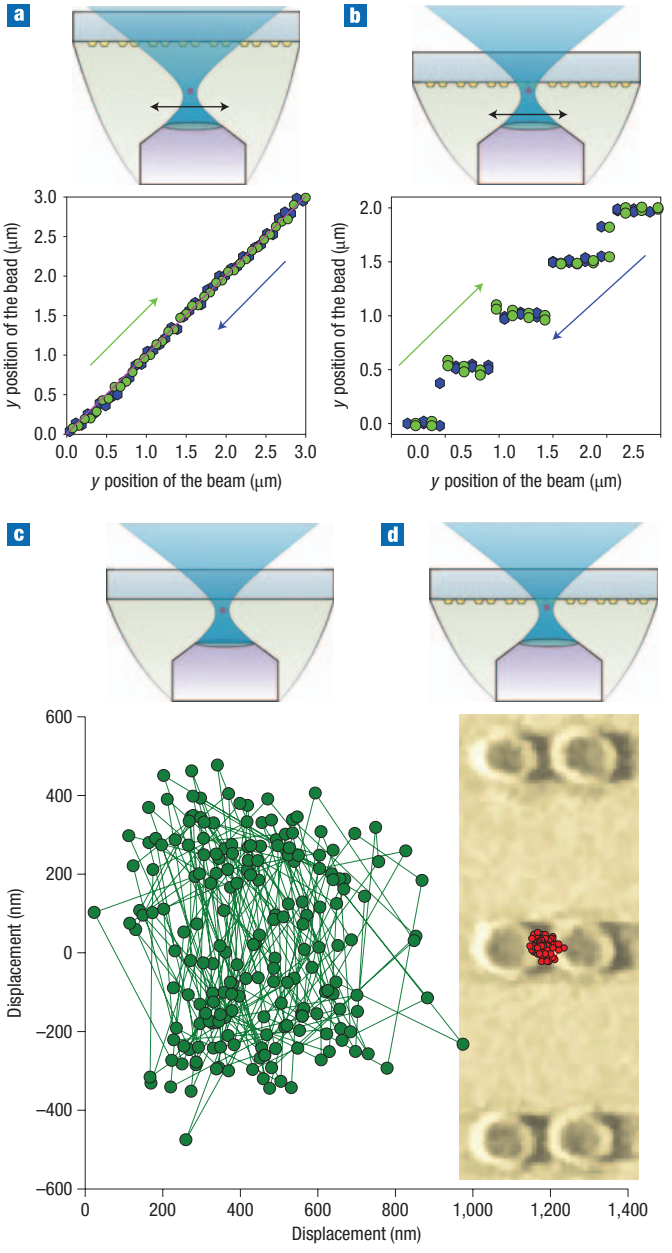

Figure 3 Nanometric trapping and quenching of brownian motion near the nanostructured substrate. a,**b**, The *y* position of a 200 nm bead as a function of the *y* position of the beam focus moving at a distance $a = 14\ \mu m$ (**a**) and $a = 0.7\ \mu m$ (**b**) from the substrate. Insets show the experimental geometry. Green and blue arrows indicate the *y* direction of motion for the laser trap (with a speed of $4\ \mu m\ s^{-1}$). Green circles correspond to positive motion, blue hexagons to negative. (The graph is shown for two cycles of motion.) **c**,**d**, Bead position as a function of time (time step, 5 ms) at a fixed position $a = 0.7\ \mu m$ of the beam focus above glass (green circles, **c**), and a nanodot pair (red circles, **d**). Insets show relevant geometries of the experiment. The electron micrograph of the sample is scaled to demonstrate the amplitude of the brownian motion with respect to the size of double-dot nanomolecules.

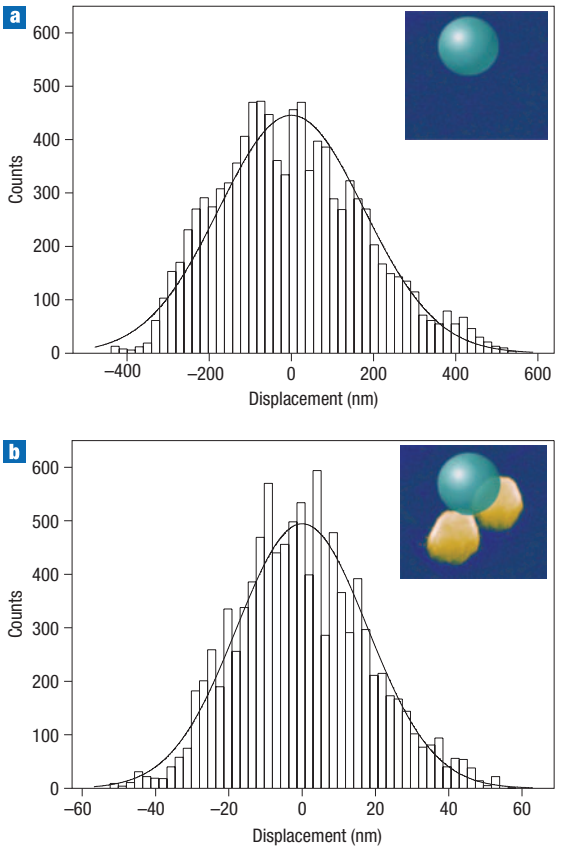

Figure 4 Histogram of particle displacement for the trapping shown in Fig. 3. a, Trapping near the glass shown in Fig. 3c. **b**, Trapping near the nanostructure shown in Fig. 3d. The solid lines in **a** and **b** represent the gaussian fits to the histograms, which gives the average displacements. The insets show the micrograph image of the pillar pair observed using an electron beam microscope under tilted angle in false colour combined with a schematic picture of the bead.

suggests a subwavelength size for the near-field trap and implies large stiffness of the trap realized near the nanodots. This has a major influence on the brownian motion of the trapped nanoparticle. In conventional optical tweezers, trapped objects are often subject to prominent brownian motion, which does not allow pinning of the position of a bead with a high precision at low laser powers. Brownian motion of a 200 nm bead outside the patterned area is shown in Fig. 3c. The plot illustrates the position of a bead trapped at $a = 0.7\ \mu m$ above the glass, measured at different times for a fixed location of the optical trap with full bandwidth of 10 kHz (green circles). Figure 3c and Fig. 4a reveal that the half-width of the gaussian distribution of displacements of a 200 nm bead was 176 nm. However, when the laser beam with the same bead (at the same power) was positioned at the same height $a = 0.7\ \mu m$ directly above the nanopillar pair, the half-width dramatically reduced to 18 nm (see the red circles of Fig. 3d; see also Fig. 4b). Figure 4 presents the histograms of the particle displacements shown in Fig. 3c,d and the corresponding gaussian fits that were used to measure the variance of the brownian motion. These variances correspond to a respective increase of the well stiffness from $1.0 \times 10^{-4}\ pN\ nm^{-1}$ to $1.3 \times 10^{-2}\ pN\ nm^{-1}$. (See Supplementary Information, movies, for examples of nanotweezers in operation, illustrating the suppression of brownian motion near the nanostructured substrate as well as the step-like manner of the bead motion between near-field traps.)

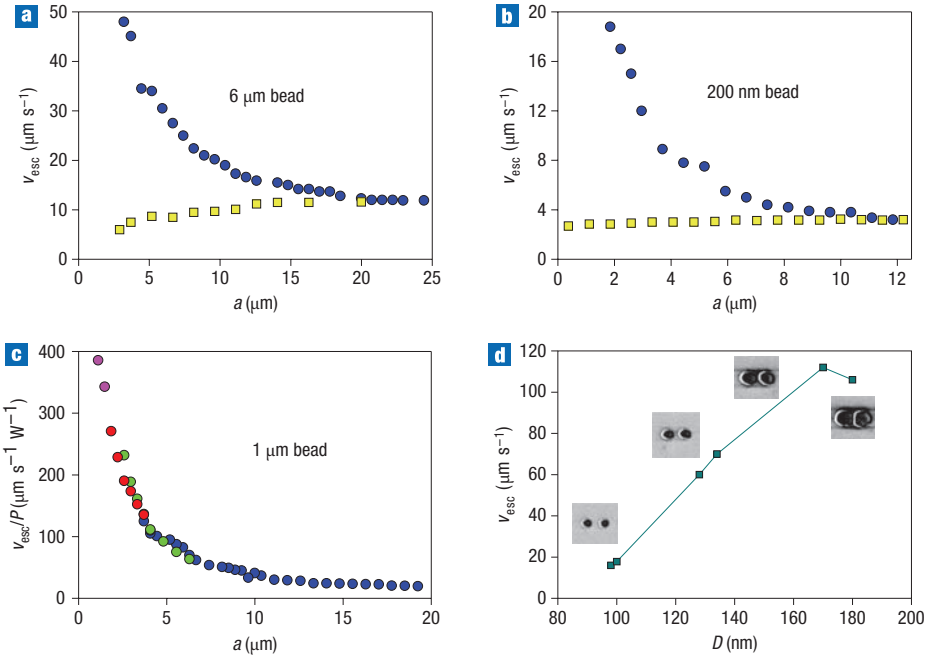

Figure 5 Escape speeds for trapped beads. **a**,**b**, Escape speed as a function of the distance a between the focus of the beam and the substrate (yellow squares for the glass substrate and blue circles for the nanostructured substrate) with nanodots of $D = 134$ nm for 6 μm beads at laser power $P = 532$ mW (**a**) and 200 nm beads at $P = 155$ mW (**b**). **c**, Ratio of the escape speed and light power (directly proportional to the quality factor Q) measured for 1 μm beads at $P = 1$ W (blue circles), $P = 440$ mW (green circles), $P = 250$ mW (red circles) and $P = 170$ mW (pink circles) as a function of distance a for nanodots of $D = 134$ nm. **d**, Escape speed as a function of nanodot diameter measured at $a = 2.5$ μm and $P = 440$ mW for a 1 μm bead. The standard error of speed measurements was $\pm 8\%$. The insets are the micrographs of a nanopillar pair for four samples. (The distance between the trapped bead and the sample surface can be less than a due to the contribution of the fields produced by the nanodots, and changes periodically when the particle moves along the sample.)

The nanodot array, therefore, provides almost an order of magnitude improvement of particle positioning with respect to conventional optical tweezers (under the same trapping conditions, that is, the same laser power). Figures 3 and 4 show that a 200 nm bead can be pinned in a near-field subwavelength trap above any illuminated nanodot pair in the array and can be moved from one double-pillar nanomolecule to another one simply by moving the beam along the array. It implies that a lattice of nanodots provides a rigid set of subwavelength near-field traps in which the particle can be positioned with very high accuracy. Such accuracy is essential in future uses, for example, for achieving reproducibility of the surface-enhanced Raman measurements that rely on the positioning of studied particles with respect to surface-enhanced Raman substrates (SERS) or for an initiation of chemical/biological reactions involving mesoscopic objects. In addition to nanometric object positioning, our structures can be simultaneously used as SERS[25].

ESCAPE-VELOCITY MEASUREMENTS

An important possibility that must be considered, however, is that the reduction in the brownian motion of a trapped particle could be due to a mechanical pinning by the substrate. In order to test this, we have measured the escape velocity of the particle from the laser beam moving above our samples. In these experiments, the particle was transported along the array of nanostructures (or a glass surface) by the laser beam, whose focal point was moved at a constant distance a above the stationary substrate along the sample surface. During its motion above the nanostructured array, the laser beam illuminated subsequent dot pairs, generating additional strong near-field forces. The near-field trap moved from one illuminated pair to the next illuminated pair when the laser beam was moved along the sample at a constant speed. We have measured experimentally the speed at which the particle was not able to follow the laser beam and escape it. The escape speed allows us to characterize an effective increase of the trapping force due to the periodic array of nanodots. Figure 5a–c shows a remarkable dependence of the escape speed of trapped beads on the distance a. As a particle is moved at smaller a along the flat glass substrate, the escape velocity is always seen to decrease and this drop is connected to the increase of the drag force near the interface arising due to an additional friction between liquid and the substrate. The drop in the escape speed was indeed observed in our experiments for beads moving near the surface of the empty glass substrate (see the yellow squares of Fig. 5a,b). Despite this growth of the drag force in the vicinity of the interface, the escape speed measured near the nanostructured sample dramatically increased for small a; see the blue circles of Fig. 5a,b, which shows $\sim$7–10 times increase in the escape speed near the nanostructured surface for beads of 6 μm and 200 nm in diameter (the data are shown for the distances where warming was not significant for the laser power used; see below). This implies that the nanostructured material increases the average force of the optical trap (by which we mean the force of the trap averaged over different beam positions within the nanoarray) by $\sim$10 times at small a, compared with a conventional optical trap. The effective trapping force F_{tr} can be evaluated directly from the escape velocity[31]. At the escape velocity, the effective trapping force is considered to be equal to the viscous drag force described by the modified Stokes law $F_d = K \cdot 6\pi\eta r v_{esc}$, where η is oil viscosity, r is the bead radius, v_{esc} the escape speed of the

particle, and $K = K(r/a)$ is a dimensionless correction coefficient[31,32]. This effective trapping force describes an average enhancement of the trapping characteristics due to near-fields in the most common applications of particles moved along the nanostructured substrate. (The discussion of the maximal value of the near-field trap for an individual dot pair will be given in future publications.) The escape velocities were equally enhanced for the trap moving in the x and y directions (that is, parallel and perpendicular to the line connecting adjacent dot centres). The data in Fig. 5 are given for the case of y motion. The maximum observed escape velocity for 1 μm beads moving in the immersion oil near the nanostructured substrate was 150 μm s^{-1}, which is extraordinarily high for motion in viscous oil and more common for the motion of trapped particles in water. Such speeds correspond to an extremely large trapping force of $F_{tr} \approx 2$nN and a large trapping efficiency 2 pN mW^{-1} calculated for a 1 μm bead near the surface. The magnitude of enhancement is extraordinary taking into account the fact that the refractive index of the bead ($n = 1.6$) is very close to the refractive index of the liquid ($n = 1.5$).

STUDIES OF THE TRAPPING QUALITY

Measurements of the escape speed allowed us to verify the significant influence of nanostructured substrates on another important characteristic of optical nanotweezers—the effective trapping quality factor defined as $Q = F_{tr}c/nP$, where c is the speed of light and n is the refractive index of the oil. (Here we chose the Minkowski form of the electromagnetic tensor only for evaluation purposes.) Figure 5c depicts a plot of the ratio of the escape velocity with the laser power v_{esc}/P measured at several different laser powers for 1 μm particles (the laser power was decreased for small a to avoid heating). The ratio v_{esc}/P is directly proportional to the quality factor Q of the optical trap (renormalized by the modified Stokes law and the modulated motion of the bead). Figure 5c clearly shows that the nanostructured substrate significantly increases the renormalized quality of the optical trap. As a result, the effective quality factor of the trap at the trapping distance of $a = 1$ μm (beads of 1 μm) from the sample surface was about 30 times higher than that of conventional tweezers without the nanostructured substrate. The calculations yield large effective trapping quality factors of $Q = 14.0 \pm 1.1$, 1.6 ± 0.13 and 0.1 ± 0.02 for 6 μm, 1 μm and 200 nm beads, respectively, near the nanostructured substrates. The escape speeds (and hence the effective trapping force) also showed a relatively strong dependence on the nanomolecule geometry—nanopillar diameter in our case—which affects the localized shape of the plasmonic resonances of the structure and influences near-field coupling in the pillar pair. Figure 5d displays the escape velocities for all six studied samples measured at a fixed laser power $P = 440$ mW for 1 μm beads at a distance of 2.5 μm from the surface of the sample. The dependence has a broad maximum for $D = 170$ nm, which we believe corresponds to the best coupling of the symmetric plasmonic mode with laser light. At the same time, a dramatic improvement of the tweezing operation has been observed even for structures with detuned shape plasmonic resonances, which should be expected for the localized plasmon resonances studied here[14]. An analogous behaviour has been observed for trapping of the microbubbles near the surface of nanostructured gold[33].

It is important to stress that the presented data have been obtained in the absence of significant heating (responsible for liquid convection and a change of immersion oil viscosity). We took several precautions to avoid heating. First, we performed our measurements at laser powers and distances a where convection, which indicates heating, was not visible. Second, we investigated the likelihood of liquid warming by measuring the dependence of the escape velocity on the trap power (which should be strongly nonlinear if significant warming is present). We found that for the distances $a \geq 2$–3 μm this dependence follows an empirical linear expression $v_{esc}(P) = \kappa(a)(P - P_0(a))$ for the powers $P < 600$ mW, where $\kappa(a)$ is a coefficient proportional to the trap quality factor and $P_0(a)$ is a threshold. For smaller distances ($a < 2$ μm) we reduced the laser power accordingly (Fig. 5c). The significant quenching of the brownian motion above the nanopillar trap shown in Fig. 3 is another convincing argument in favour of the absence of heating. Indeed, the oil viscosity η strongly depends on temperature. Because the brownian motion is inversely proportional to oil viscosity (the power spectrum for a trapped overdamped bead can be evaluated as $S(f) = kT/(6\pi^3 rf^2\eta)$, where f is the frequency and T is the temperature), it implies that oil heating would dramatically increase the particle brownian motion, but experiments unambiguously show a significant decrease of brownian wandering of a bead above the nanodot trap.

DISCUSSION

To conclude, we have demonstrated a subwavelength near-field optical tweezer system created near a nanostructured substrate. The proposed nanotweezers provide a set of 'absolute' discrete coordinates in which optical near-fields of nanopillars provide a subwavelength trapping volume for the trapped nanoparticles and open new exciting possibilities in different fields of science and nanotechnology. The system could be easily developed to allow an interrogation of many nanomolecules at once (and establishing a long-range order in a solution) by using light beams with a broader gaussian waist. The enhanced characteristics of optical nanotweezers could provide an instrumental edge in the field of nanoengineering and open new avenues for nanophysics and nanobiology.

METHODS

The nanostructured samples were produced by electron beam lithography. The studied arrays of gold nanopillars had periods from 270 to 600 nm, dot diameters of 100–140 nm, and pillar separations in the pair were 140–200 nm. The optical tweezers set-up has been described in detail previously[29]. The escape velocities and measurements of the quantized motion of the particles above the nanoarray were obtained for the particles transported by moving the beam focus in the x–y plane using the galvanometer-controlled mirrors. Calibrations of the x–y stage were checked during the experiments and the motorized z drive of the microscope focus was calibrated interferometrically before experiments. Relative measurements of the focus height above the nanopillars were set by observing the speckle reflection of the trapping beam from the structures and setting this position to the 0 value of the z coordinate. A new addition to the tweezer apparatus was the quadrant photodiode (QPD). The QPD was used and calibrated as described by Pralle *et al.*[34]. Particle tracking was accomplished using a 632.8 nm HeNe laser with a bandpass filter at the QPD used to remove any contribution from the trapping laser and nanosubstrate. Furthermore, a dark-field scheme was used to improve the signal-to-noise ratio. The presence of nanodots made it difficult to deduce the particle motion normal to the substrate from the total scattering. The video imaging system used the ordinary microscope set-up with a short pass filter to filter the 1,064 nm beam at the camera.

Received 1 November 2007; accepted 17 March 2008; published 11 May 2008.

References

1. Eigler, D. M. & Schweizer, E. K. Positioning single atoms with a scanning tunnelling microscope. *Nature* **344,** 524–526 (2000).
2. Bustamante, C., Bryant, Z. & Smith, S. B. Ten years of tension: single-molecule DNA mechanics. *Nature* **421,** 423–427 (2003).

3. Lewis, A. *et al.* Near-field optics: From subwavelength illumination to nanometric shadowing. *Nature Biotechnol.* **21,** 1378–1386 (2003).
4. Ashkin, A., Dziedzic, J. M., Bjorkholm, J. E. & Chu, S. Observation of a single-beam gradient force optical trap for dielectric particles. *Opt. Lett.* **11,** 288–290 (1986).
5. Grier, D. G. A revolution in optical manipulation. *Nature* **424,** 810–816 (2003).
6. Crocker, J. C. & Grier, D. G. When like charges attract: The effects of geometrical confinement on long-range colloidal interactions. *Phys. Rev. Lett.* **77,** 1897–1900 (1996).
7. Wang, G. M., Sevick, E. M., Mittag, E., Searles, D. J. & Evans, D. J. Experimental demonstration of violations of the second law of thermodynamics for small systems and short time scales. *Phys. Rev. Lett.* **89,** 050601 (2002).
8. Cran-McGreehin, S. J., Dholakia, K. & Krauss T. F. Monolithic integration of microfluidic channels and semiconductor lasers. *Opt. Express* **14,** 7723–7729 (2006).
9. Molloy, J. E. & Padgett, M. J. Lights, action: optical tweezers. *Cont. Phys.* **43,** 241–258 (2002).
10. Neuman, K. C. & Block, S. M. Optical trapping. *Rev. Sci. Instrum.* **75,** 2787–2809 (2004).
11. Dholakia, K. & Reece, P. Optical manipulation takes hold. *Nano Today* **1,** 18–27 (2006).
12. Abbondanzieri, E. A., Greenleaf, W. J., Shaevitz, J., Landick, W.R. & Block, S. M. Direct observation of base-pair stepping by RNA polymerase. *Nature* **438,** 460–465 (2005).
13. Born, M. & Wolf, E. *Principles of Optics* (Cambridge Univ. Press, Cambridge, 1999).
14. Grigorenko, A. N. *et al.* Nanofabricated media with negative magnetic permeability at visible frequencies. Nature **438,** 335–338 (2005).
15. Betzig, E. & Trautman, J. K. Near-field optics: microscopy, spectroscopy and surface modification beyond the diffraction limit. *Science* **257,** 189–195 (1992).
16. Ebbesen, T. W., Lezec, H. J., Ghaemi, H. F., Thio, T. & Wolff, P. A. Extraordinary optical transmission through subwavelength hole arrays. *Nature* **391,** 667–669 (1998).
17. Fang, N., Lee, H., Sun, C. & Zhang, X. Sub-diffraction-limited optical imaging with a silver superlens. *Science* **308,** 534–537 (2005).
18. Kawata, S. & Sugiura, T. Movement of micrometer-sized particles in the evanescent field of a laser beam. *Opt. Lett.* **17,** 772–774 (1992).
19. Novotny, L., Bian, R. X. & Xie, X. S. Theory of nanometric optical tweezers. *Phys. Rev. Lett.* **79,** 645–648 (1997).
20. Quidant, R., Petrov, D. & Badenes, G. Radiation forces on a Rayleigh dielectric sphere in a patterned optical near field. *Opt. Lett.* **30,** 1009–1011 (2005).
21. Volpe, G., Quidant, R., Badenes, G. & Petrov, D. Surface plasmon radiation forces. *Phys. Rev. Lett.* **96,**, 238101 (2006).
22. Reece, P. J., Garcés-Chávez, V. & Dholakia, K. Near-field optical micromanipulation with cavity enhanced evanescent waves. *Appl. Phys. Lett.* **88,** 221116 (2006).
23. Garcés-Chávez, V. *et al.* Extended organization of colloidal microparticles by surface plasmon polariton excitation. *Phys. Rev. B* **73,** 085417 (2006).
24. Gu, M., Haumonte, J.-B., Micheau, Y., Chon, J. W. M. & Gan, X. Laser trapping and manipulation under focused evanescent wave illumination. *Appl. Phys. Lett.* **84,** 4236–4238 (2004).
25. Grigorenko, A. N. *et al.* An antisymmetric plasmon resonance in coupled gold nanoparticles as a sensitive tool for detection of local index of refraction. *Appl. Phys. Lett.* **88,** 124103 (2006).
26. Panina, L. V., Grigorenko, A. N. & Makhnovskiy, D. P. Metal–dielectric medium with conducting nanoelements. *Phys. Rev. B* **66,** 155411 (2002).
27. Su, K.-H. *et al.* Interparticle coupling effects on plasmon resonances of nanogold particles. *Nano Lett.* **3,** 1087–1090 (2003).
28. Rechberger, W. *et al.* Optical properties of two interacting gold nanoparticles. *Opt. Commun.* **220,** 137–141 (2003).
29. Wright, A. J., Wood, T. A., Dickinson, M. R., Gleeson, H. F. & Mullin, T. The transverse trapping force of an optical trap: factors affecting its measurement. *J. Mod. Opt.* **50,** 1521–1532 (2003).
30. Kuiru, L., Stockman, M. I. & Bergman, D. J. Self-similar chain of metal nanospheres as an efficient nanolens. *Phys. Rev. Lett.* **91,** 227402 (2003).
31. Wright, W. H., Sonek, G. J. & Berns, M. W. Parametric study of the forces on microspheres held by optical tweezers. *Appl.Opt.* **33,** 1735–1748 (1994).
32. Happell, J. & Brenner, H. *Low Reynolds Number Hydrodynamics with Special Applications to Particulate Media* (Prentice Hall, Englewood Cliffs, NJ, 1965).
33. Sidorov, A. R., Zhang, Y., Grigorenko, A. N. & Dickinson, M. R. Nanometric optical tweezers based on nanostructured substrates. *Opt. Commun.* **278,** 439–444 (2007).
34. Pralle, A., Prummer, M., Florin, E.-L., Stelzer, E. H. K. & Horber, J. K. H. Three-dimensional high resolution particle tracking for optical tweezers by forward scattered light. *Microsc. Res. Technique* **44,** 378–386 (1999).

Supplementary Information accompanies this paper at www.nature.com/naturephotonics.

Acknowledgements

This research was supported by EPSRC (UK) and the Paul Instrument Fund. We thank H. F. Gleeson for kind permission to use the optical tweezers set-up.

Author information

Reprints and permission information is available online at http://npg.nature.com/reprintsandpermissions/.
Correspondence and requests for materials should be addressed to A.N.G.